

First radical cation salt of bis(ethylenedithio)tetrathiafulvalene with organic anion $[\text{C}(\text{NCN})_2\text{NH}_2]^-$: synthesis, structure, and conducting properties

N. D. Kushch,^{a*} N. G. Spitsina,^a A. M. Kolesnikova,^a and S. V. Simonov^b

^aInstitute of Problems of Chemical Physics, Russian Academy of Sciences,
1 prosp. Akad. Semenova, 142432 Chernogolovka, Moscow Region, Russian Federation.
Fax: +7 (496) 522 3507. E-mail: kushch@icp.ac.ru

^bInstitute of Solid State Physics, Russian Academy of Sciences,
2 ul. Akad. Osip'yana, 142432 Chernogolovka, Moscow Region, Russian Federation.
Fax: +7 (496) 522 8160

The electrochemical oxidation of bis(ethylenedithio)tetrathiafulvalene (ET) in the presence of simple dicyanamide salts of rare-earth metals with the general formula $\text{M}[\text{N}(\text{CN})_2]_3$ ($\text{M} = \text{Gd}^{3+}$, Dy^{3+} , and Ho^{3+}) as electrolytes was studied for the first time. A novel radical-cation salt $\alpha\text{-ET}_2[\text{C}(\text{NCN})_2\text{NH}_2]$ with the unexpected (2,1-dicyano)guanidine anion was synthesized. The crystal structure of the salt and its conducting properties were studied. The structure of the salt is layered with alternating conducting radical-cation and insulating anionic layers. The cationic layers of the α -type are formed by two crystallographically independent radical-cations of ET of various charges. The anionic layers are formed of $[\text{C}(\text{NCN})_2\text{NH}_2]^-$ anions linked by hydrogen contacts into chains. The crystals of $\text{ET}_2[\text{C}(\text{NCN})_2\text{NH}_2]$ demonstrate a semiconducting character of conductivity in a temperature range of 300–100 K.

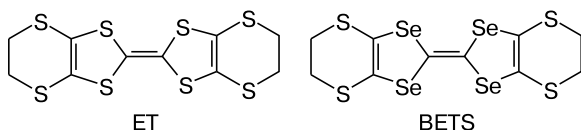
Key words: radical-cation salt, bis(ethylenedithio)tetrathiafulvalene, dicyanamide salts of rare-earth metals, electrocrystallization, structure, conductivity.

A novel scientific trend related to the production of bi(multi)functional materials appeared in the recent 10–15 years in the chemistry and physics of radical-cation salts based on chalcogen-containing π -donors. The structures of these materials are formed by two spatially separated subsystems, each of which exhibits different properties, for example, such as conductivity and photochromism, conductivity and magnetism.^{1,2} The works on the synthesis and study of bifunctional molecular compounds combining the conducting and magnetic properties have been carried out most actively in the recent time. At the moment, investigations in this direction are concentrated on the family of low-dimensional conductors based on radical-cation salts with paramagnetic anionic complexes.¹ In these materials the conductivity is related to electrons in organic layers, whereas the magnetic properties are usually determined by localized ions of transition metals in insulating layers. In particular, the coexistence of superconducting and paramagnetic properties^{2–4} or even antiferromagnetic properties^{5–7} was found in salts of bis(ethylenedithio)tetrathiafulvalene (ET) and bis(ethylenedithio)tetraselenafulvalene (BETS). Moreover, it was found that the interaction of localized spins in insulating layers with π -electrons in conducting layers can result in such an unusual phenomenon as superconductiv-

ity induced by magnetic field, which was observed in crystals of $\kappa\text{-(BETS)}_2\text{FeCl}_4$ and $\kappa\text{-(BETS)}_2\text{FeBr}_4$.^{8,9}

A combination of conducting and magnetic subsystems in crystals of the radical-cation salts and various manifestations of synergetic effects also can favor the appearance of new properties. In addition to traditionally used halide, cyanide, and oxalate transition metal complexes, dicyanamido metallates recently attract researchers attention as magnetic counterions in radical-cation salts.^{10–12} These complexes are characterized by a great variety of structures and exhibit diverse magnetic properties (ferromagnetism, antiferromagnetism, and paramagnetism), which depend on the character of exchange interactions between unpaired d-electrons of the metal atoms through the bridging ligands $\text{N}(\text{CN})_2^-$. A relationship between the nature of the d-metal and composition of the synthesized radical-cation salts was found by the study of the electrochemical oxidation of ET in the presence of dicyanamides of d-metals (Mn^{2+} , Co^{2+} , Cr^{3+} , and Cu^{2+}) as electrolytes. It was established that different products were obtained depending in the metal nature.^{10–18} However, only the use of dicyanamidomanganates in the form of simple ($\text{Mn}[\text{N}(\text{CN})_2]_2$) or complex ($\text{Ph}_4\text{P}\{\text{Mn}[\text{N}(\text{CN})_2]_3\}$) salt as electrolytes resulted in the formation of crystals with dicyanamidometallate anions: $(\text{ET})_2\{\text{Mn}[\text{N}(\text{CN})_2]_3\}$ and

and $(ET)_2\{MnCu[N(CN)_2]_4\}$.^{11,14} We have recently synthesized a novel radical-cation salt based on the BETS donor (κ -BETS₂{Mn[N(CN)₂]₃}), which combines the superconducting ($T_c = 5.75$ K at $P = 0.4$ Kbar) and antiferromagnetic properties.¹⁹ Relationships were observed in this salt between the metal—dielectric phase transition in the conducting BETS subsystem and the formation of the short-range magnetic order in insulating anionic layers in the range of the temperature of the metal—insulator transition.^{19,20} As established later, the metal—dielectric transition is also accompanied by the antiferromagnetic transition in the conducting sublattice.²¹



The study of magnetic dicyanamides of rare-earth 4f-elements as magnetic counterions is of special interest. Unlike d-metals, 4f-elements are characterized by high anisotropy of magnetic properties and a higher coordination number in complex salts and exhibit luminescence properties. The appearance of new properties cannot be excluded in radical-cation salts with anions of this type.

In this work, we studied the electrochemical oxidation of ET in the presence of simple dicyanamide salts of rare-earth metals (REM) with the general formula $M[N(CN)_2]_3$ ($M = Gd, Dy, Ho$) as electrolytes. Radical-cation salt $ET_2[C(NCN)_2NH_2]$ (**1**) with the unexpected (2,1-dicyano)guanidine anions $[C(NCN)_2NH_2]^-$ was synthesized for the first time, and its crystal structure and conducting properties were studied.

Results and Discussion

The electrochemical oxidation of ET was carried out in various solvents (dichloromethane—EtOH (96%), 1,1,2-trichloroethane—EtOH (96%), chlorobenzene—EtOH(abs.)) in the presence of simple salts of REM dicyanamides with the general formula $M[N(CN)_2]_3 \cdot 2H_2O$ ($M = Gd, Dy, Ho$). Two-component mixtures $(Ph_4P)[N(CN)_2] + M[N(CN)_2]_3 \cdot 2H_2O$ (1 : 1) were stud-

ied as electrolytes. When $Ho[N(CN)_2]_3 \cdot 2H_2O + (Ph_4P)[N(CN)_2]$ (1 : 1) mixture is used as an electrolyte, orthorhombic crystals of radical-cation salt **1** are formed having the counterion $[C(NCN)_2NH_2]^-$, which differs from the starting anion in the electrolyte. The introduction of simple salts of Gd^{3+} or Dy^{3+} dicyanamides into the electrolyte under similar synthesis conditions is accompanied by the growth of crystals of an organic conductor of the known structure, *viz.*, bis(ethylenedithio)tetrathiafulvalene dicyanamide dihydrate (α'' - $ET_2N(CN)_2 \cdot 2H_2O$, **2**).¹⁸ The formation of crystals of this salt could be assumed on the basis of the dissociation of the electrolyte components in the solution to form $N(CN)_2^-$ anion. The latter can participate in the formation of both metallo-complex anions Ho^{3+} (in particular, $\{Ho[N(CN)_2]_6\}^{3-}$) and related radical-cation salts and radical-cation salts containing no metals. However, the presence of the $[C(NCN)_2NH_2]^-$ ion in the salt was quite unexpected. We have previously found that crystals of salt α''' - $(ET)_6(NO_3)_3 \cdot 2(C_2H_5O_2N_3)$ containing two biuret ($C_2H_5O_2N_3$) molecules were grown during the electrochemical oxidation of ET in the presence of electrolyte $Cr[N(CN)_2]_{1.5}(NO_3)_{1.5} \cdot 6H_2O$ instead of the expected radical-cation salt with the metallocomplex anion.¹⁸ As shown earlier,¹⁶ the formation of biuret molecules is a result of hydrolysis of the terminal $-C\equiv N$ groups of the dicyanamide anion. In this case, the formation of anion $[C(NCN)_2NH_2]^-$ upon the electrocrystallization of ET in the presence of the simple holmium salt as an electrolyte is also related, probably, to the hydrolysis of the $-C\equiv N$ groups of the $[N(CN)_2]^-$ anion followed by condensation presumably *via* Scheme 1.

The optimum conditions for crystal growth of salts **1** and **2** are given in Experimental. The absence of metals in the composition of radical-cation salts **1** and **2** were preliminarily established by electron-probe X-ray spectral microanalysis (EPMA). The final compositions of both salts were found by the full X-ray diffraction analysis. The main crystallographic data and structure refinement parameters for salt **1** are presented in Table 1.

The crystals of **1** have a non-centrosymmetric layered structure in which conducting radical-cation layers alternate with insulating anionic layers along the direction of

Scheme 1

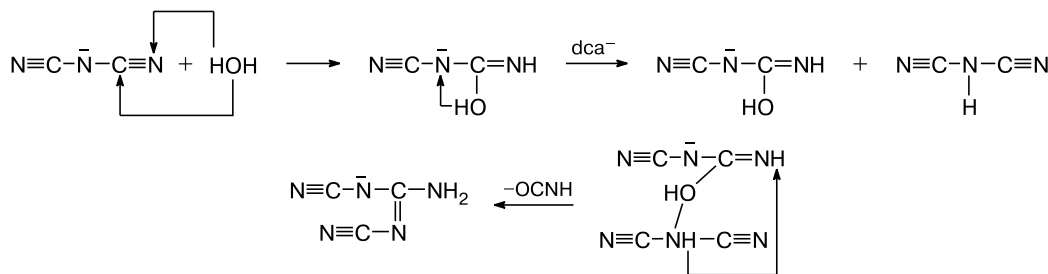
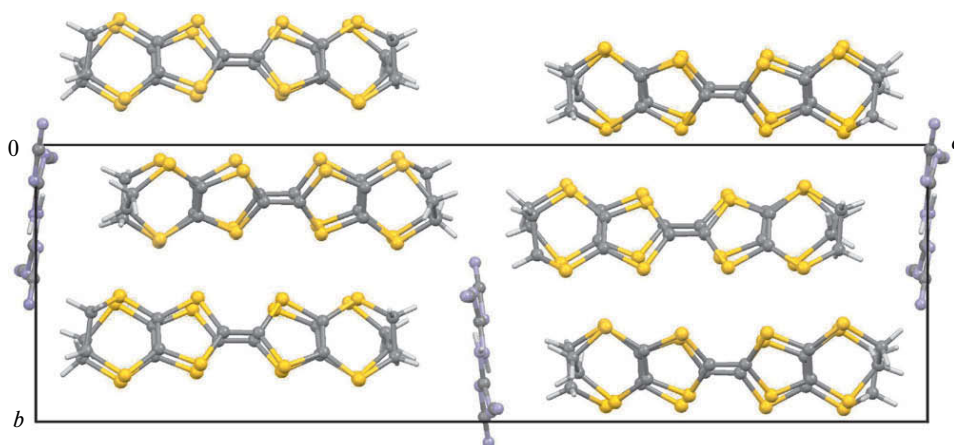


Table 1. Main crystallographic data and refinement parameters for the structure of salt $(\text{ET})_2[\text{C}(\text{NCN})_2\cdot\text{NH}_2]$

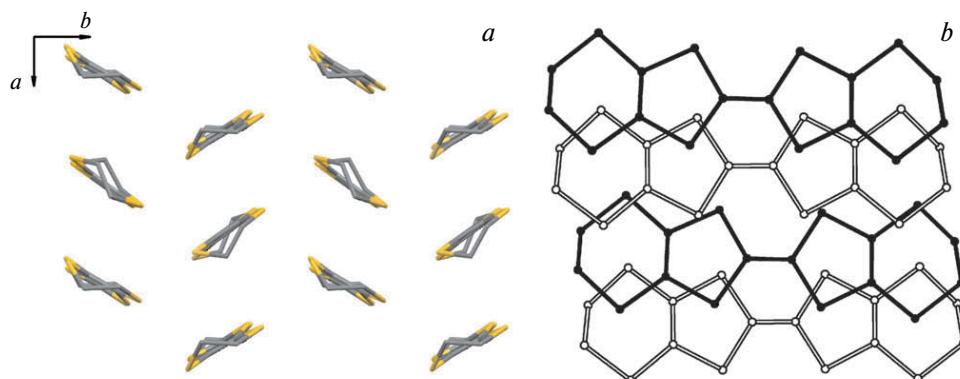
Parameters	1
Formula	$\text{C}_{23}\text{H}_{18}\text{N}_5\text{S}_{16}$
Molecular weight	877.38
Crystal system	Orthorhombic
Space group	$P2_12_12_1$
$a/\text{\AA}$	9.2417(7)
$b/\text{\AA}$	10.5926(5)
$c/\text{\AA}$	34.113(1)
α/deg	90
β/deg	90
γ/deg	90
$V/\text{\AA}^3$	3339.5(3)
Z	4
$d_{\text{calc}}/\text{g cm}^{-3}$	1.745
μ/cm^{-1}	1.064
Scan mode	2–30.5
Number of measured reflections (R_{int})	48178 (0.038)
Number of independent reflections with $I > 2\sigma(I)$	10180 9532
Number of refined parameters	398
R_1 ($I > 2\sigma(I)$)	0.033
ωR_2 (for all reflections)	0.077

the c axis (Fig. 1). Two conducting layers per unit cell are related to each other by the symmetry axis 2_1 . The radical-cation layers of the α -type are formed by symmetrically dependent stacks of ET molecules. The stack is formed by two crystallographically independent radical-cations **A** and **B** alternating along the a axis (Fig. 2, *a*). The numeration of atoms in the structure of this salt is presented in Fig. 3. The angle between the central 1,4-dithione (TTF) fragments of adjacent molecules **A** and **B** in the stack is $5.25(1)^\circ$. This is a distinctive feature of the radical-cation layer in salt **1** unlike the most part of radical-cation salts with the packing of the α -type in which the donor molecules in the stack are mutually parallel.²² The planes of the radical cations are inclined relative to the direction of stack (a axis) at an angle of $50.09(1)^\circ$ and $53.89(1)^\circ$ for **A** and **B**, respectively. The central TTF fragments of symmetrically dependent donors from the adjacent stacks have an inclination of $114.14(1)^\circ$. The overlap of the radical cations in the stack is of the "ring above atom" type for which the donor molecules are shifted relative to each other in the cross direction (see Fig. 2, *b*). The intermolecular distances in the stack are $3.8(1)$ and $3.7(1)$ \AA .

According to the stoichiometry, each radical-cation $\text{ET}^{\cdot+}$ should have the charge equal to $+0.5$. A comparison

**Fig. 1.** Projection of the crystal structure of salt $\text{ET}_2[\text{C}(\text{NCN})_2\text{NH}_2]$ along the a direction.

Note. Figures 1, 2, and 4 are available in full color in the on-line version on the web-page (<http://www.link.springer.com>).

**Fig. 2.** *a*, Projection of the radical-cation layer along the major axis of the molecule. *b*, Overlaps of the molecules in the stack of salt $\text{ET}_2[\text{C}(\text{NCN})_2\text{NH}_2]$. Thermal ellipsoids of $\sim 50\%$ probability.

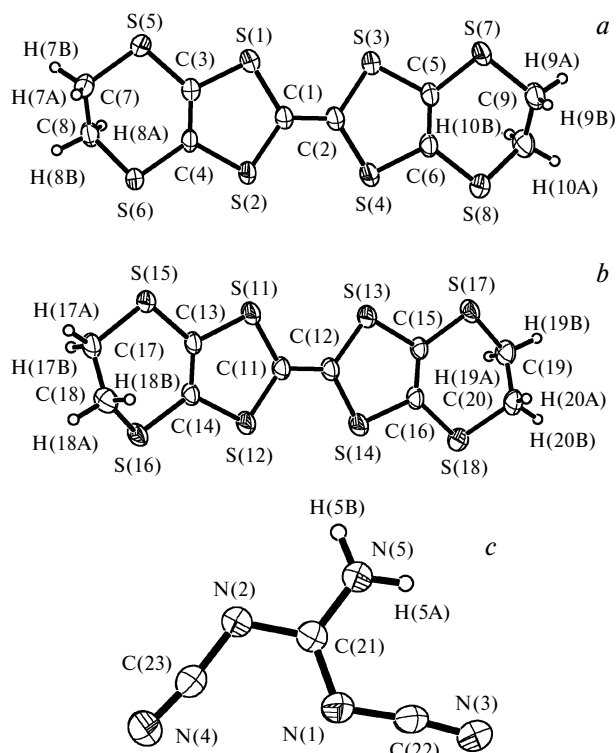


Fig. 3. Numeration of atoms in radical-cations **A** (a) and **B** (b) and in anion $[\text{C}(\text{NCN})_2\text{NH}_2]^-$ (c) in salt $\text{ET}_2[\text{C}(\text{NCN})_2\text{NH}_2]$. Thermal ellipsoids are presented with 50% probability.

of the bond lengths of the central TTF fragment ($\text{C}(1) - \text{C}(2) = 1.357(3) \text{ \AA}$, $\text{C}(11) - \text{C}(12) = 1.390(2) \text{ \AA}$) shows that radical-cation **A** has a charge close to ET^0 , and that of **B** is close to $\text{ET}^{+\cdot}$. The charge calculated by the empirical equation²³ gives values of +0.26 and +0.99 for donor molecules **A** and **B**, respectively. The dihedral angles between the (S_4C_2) fragments with the edges passing along the $\text{S}(1) - \text{S}(2)$ and $\text{S}(3) - \text{S}(4)$ bonds for molecules **A** and along the $\text{S}(11) - \text{S}(12)$ and $\text{S}(13) - \text{S}(14)$ bonds for molecules **B** are $7.59(2)^\circ$ and $6.22(2)^\circ$, respectively, vs $3.77(1)^\circ$ and $2.32(1)^\circ$. Molecules **A** and **B** are characterized by a "boat" conformation. The terminal ethylene groups in both radical-cations have a eclipsed conformation. The conducting layer contains a series of shortened contacts of the $\text{S} \dots \text{S}$ and $\text{S} \dots \text{C}$ types between the adjacent ET molecules. The values of the contacts are given in Table 2.

The anionic layer in the crystals of salt **1** consists of double chains formed along the a direction of the planar $[\text{C}(\text{NCN})_2\text{NH}_2]^-$ anions in which the anions are linked by hydrogen bonds $\text{N} - \text{H} \dots \text{N}$ (Fig. 4). The anion is inclined relative to the ab plane by an angle of $12.43(4)^\circ$. There are a series of shortened $\text{S} \dots \text{N}$ contacts and hydrogen bonds between the anionic and radical-cation layers. Their values are listed in Table 2.

The conductivity of the crystals of salt **1** at room temperature is $2 \cdot 10^{-2} \text{ Ohm}^{-1} \text{ cm}^{-1}$. The salt demonstrates the semiconducting character of conductivity in the tem-

Table 2. Shortened intermolecular contacts in the structure of salt $(\text{ET})_2[\text{C}(\text{NCN})_2\text{NH}_2]$

Contact	Contact length/ \AA
$\text{S}(2) - \text{S}(17)$	3.558
$\text{S}(6) - \text{S}(17)$	3.476
$\text{S}(8) - \text{S}(11)$	3.563
$\text{S}(8) - \text{S}(15)$	3.587
$\text{S}(5) - \text{S}(18)$	3.584
$\text{S}(12) - \text{S}(17)$	3.573
$\text{S}(16) - \text{S}(17)$	3.536
$\text{S}(15) - \text{S}(18)$	3.604
$\text{S}(7) - \text{S}(12)$	3.612
$\text{S}(1) - \text{S}(18)$	3.686
$\text{S}(7) - \text{S}(16)$	3.693

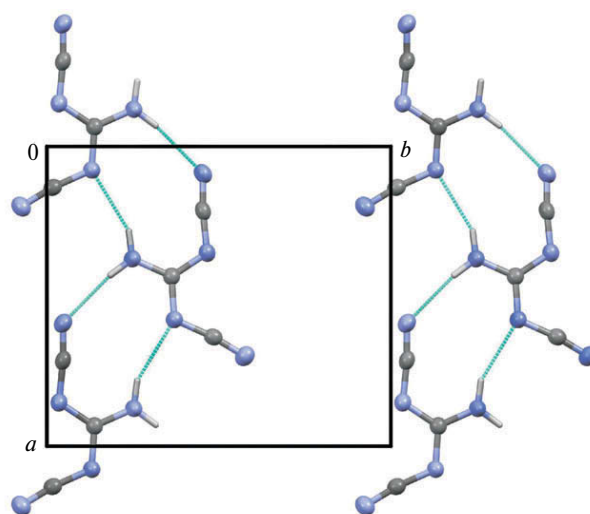


Fig. 4. Projection of the anionic layer in salt $\text{ET}_2[\text{C}(\text{NCN})_2\text{NH}_2]$.

perature range from 300 to 100 K with activation energies of 0.16 and 0.44 eV for the low- (220–140 K) and high-temperature (250–300 K) ranges respectively (Fig. 5).

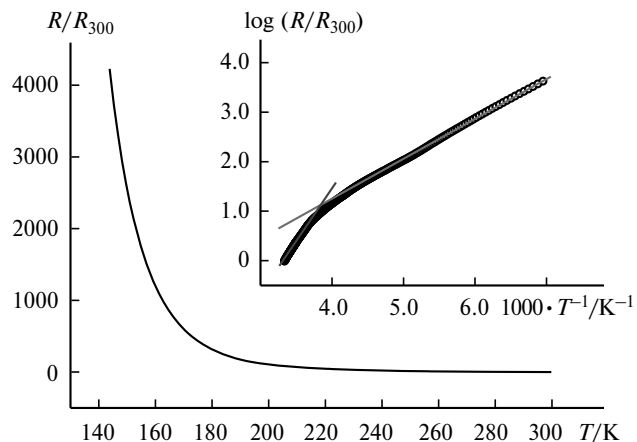


Fig. 5. Temperature dependence of the resistance for a single crystal of $\text{ET}_2[\text{C}(\text{NCN})_2\text{NH}_2]$.

This behavior corresponds to the observed charge ordering (charge localization) in the conducting layer of the crystal structure.

Experimental

Bis(ethylenedithio)tetrathiafulvalene (ET, Aldrich) was purified by recrystallization from chlorobenzene (C_6H_5Cl , Fluka), tetraphenylphosphonium bromide ($(Ph_4P)Br$, Aldrich, >99.5%), sodium dicyanamide ($Na[N(CN)_2]$, Fluka, >96%), and REM nitrate hexahydrates (Alfa Ventron, 99.9%) were used as received.

Synthesis of electrolytes and salts α - $ET_2[C(NCN)_2NH_2]$ (1**) and α '- $ET_2N(CN)_2 \cdot 2H_2O$ (**2**).** Electrolytes $M[N(CN)_2]_3 \cdot 2H_2O$ ($M = Gd, Dy, Ho$) used in the work were obtained according to a described procedure²⁴ using ion exchange in an aqueous solution at room temperature on a column containing 5 mL of the strongly acidic ion-exchange resin (Merck, Ionenaustauscher I, Art. 4765) with a capacity of 1.7 mmol mL^{-1} . A $2 \cdot 10^{-2} \text{ M}$ aqueous solution corresponding to salt $M(NO_3)_3 \cdot 6H_2O$ ($M = Gd, Dy, Ho$) was passed through a column before it was filled with metal ions. The process was monitored by a change in the pH of the eluate from acidic to neutral value. The column was washed with bidistilled water to remove an excess of REM nitrates, then a $25 \cdot 10^{-2} \text{ M}$ aqueous solution of sodium dicyanamide was passed, and the eluate was collected. After a portion of the solvent from the eluate solution was evaporated at room temperature and crystals were formed, coarse-crystalline fractions were selected and dried at 100°C to a constant weight. The energy-dispersive X-ray fluorescence analysis of $M[N(CN)_2]_3$ powders unambiguously showed the presence of the corresponding metal in the salts. The IR spectra of polycrystalline samples of $M[N(CN)_2]_3 \cdot 2H_2O$ contain absorption bands corresponding to vibrations of the $C \equiv N$, $N-C$, and $N-C \equiv N$ bonds characteristic of coordinated dicyanamide groups in the lanthanide(III) salts.²⁴ The broad absorption band in a range of $3600-3000 \text{ cm}^{-1}$ and the narrow bands at $1630-1650 \text{ cm}^{-1}$ indicate the presence of water in the salts of the general formula $M[N(CN)_2]_3 \cdot 2H_2O$ (**3**) ($M = Gd$ (**a**), Dy (**b**), and Ho (**c**)).

Elemental analysis for $Gd[N(CN)_2]_3 \cdot 2H_2O$ (**3a**). Found (%): C, 18.44; H, 1.06; N, 32.25. $GdC_6H_4N_9O_2$. Calculated (%): C, 18.40; H, 1.02; N, 32.21.

Elemental analysis for $Dy[N(CN)_2]_3 \cdot 2H_2O$ (**3b**). Found (%): C, 18.00; H, 1.07; N, 31.58. $DyC_6H_4N_9O_2$. Calculated (%): C, 17.98; H, 1.00; N, 31.46.

Elemental analysis for $Ho[N(CN)_2]_3 \cdot 2H_2O$ (**3c**). Found (%): C, 18.01; H, 1.00; N, 31.29. $HoC_6H_4N_9O_2$. Calculated (%): C, 17.92; H, 1.00; N, 31.36. The melting points of the synthesized compounds were higher than 350°C .

Compound $(Ph_4P)[N(CN)_2]$ (**4**) was synthesized according to a known procedure²⁵ by the exchange reaction mixing aqueous solutions of $(Ph_4P)Br$ and $Na[N(CN)_2]$. The clotted white precipitate formed was filtered off and washed with distilled water and diethyl ether. The product was recrystallized two times from methanol to obtain $(Ph_4P)[N(CN)_2]$ as a white powder. Found (%): C, 77.04; H, 4.94; N, 10.38. $C_{26}H_{20}N_3P$. Calculated (%): C, 77.02; H, 4.97; N, 10.37. *m.p.* $210.5-211^\circ\text{C}$.

Orthorhombic crystals of compound **1** were synthesized by the electrochemical oxidation of the donor ($C_1 = 0.12 \cdot 10^{-3} \text{ mol L}^{-1}$) in a mixture of solvents chlorobenzene—EtOH(abc.) (15 : 2, mL) at constant current ($I = 0.5 \text{ }\mu\text{A}$) and the current density

equal to $1 \text{ }\mu\text{A cm}^{-2}$ at 25°C in an argon atmosphere. A mixture of two salts, $(Ph_4P)[N(CN)_2] + Ho[N(CN)_2]_3 \cdot 2H_2O$ (1 : 1) ($C_2 = 0.5 \cdot 10^{-3} \text{ mol L}^{-1}$), was used as an electrolyte. The synthesis was carried out in a glass H-like two-electrode cell with the separated cathodic and anodic compartments. Diffusion restrictions were created with a glass porous filter no. 3. Platinum wires 1 mm in diameter served as electrodes after their preliminary electrochemical purification in a 0.1 N sulfuric acid solution. Black lustrous orthorhombic crystals $0.6 \times 0.3 \times 0.8 \text{ mm}$ in size were grown on the anode within 1.5–2 weeks. The crystals were filtered off, washed with acetone, and dried in air. The plate-like crystals of **2** were obtained using the procedure similar to the synthesis of salt **1** in the presence of the electrolyte consisting of a 1 : 1 mixture of two salts $(Ph_4P)[N(CN)_2] + M[N(CN)_2]_3 \cdot 2H_2O$ ($M = Gd, Dy$).

Energy-dispersive X-ray fluorescence analysis. The presence of rare-earth elements in the electrolytes (**3a–c**) was monitored by energy-dispersive X-ray fluorescence analysis on an X-Apt M spectrometer (COMITA, Russia) equipped with an X-ray tube with the silver anode. The presence of REM was established by L lines. The measurements for the samples containing gadolinium and dysprosium were conducted at the following parameters: voltage on the tube 15 kV, current 100 mA, and living time 60 s. The measurement parameters for the detection of holmium were as follows: voltage 25 kV, current 300 mA, and living time 60 s.

Elemental analysis and IR spectroscopy. The elemental analyses of salts $M[N(CN)_2]_3 \cdot 2H_2O$ ($M = Gd, Dy, Ho$) and $(Ph_4P)[N(CN)_2]$ were carried out on a Vario MICRO Cube analyzer.

The IR spectra of samples **3a–c** were recorded at room temperature on a Varian 3100 FT-IR spectrophotometer (EXCALIBUR SERIES) in the frequency range from 4000 to 400 cm^{-1} with the Smart HART attachment of multiple attenuated total internal reflectance on a planar crystal of ZnSe Flat without special sample preparation. Absorption bands in the IR spectra were assigned on the basis of published data.^{24,25}

Electron-probe X-ray spectral microanalysis. The preliminary compositions of single crystals of **1** and **2** were determined by the electron-probe X-ray spectral microanalysis method on a JEOL JSM-5800L scanning electron microscope with a thousand-fold magnification and an electron beam energy of 20 keV. The depth of beam penetration into the sample was $1-3 \text{ }\mu\text{m}$.

X-ray diffraction analysis. Unit cell parameters of crystals **1** and **2** and the experimental set of reflection intensities were obtained on an Oxford Diffraction GeminiR four-circle diffractometer with a CCD detector (MoK α radiation, ω scan mode, graphite monochromator) at room temperature. An absorption correction of diffraction reflection intensities was applied by the SCALE3 ABSPACK algorithm in the CrysAlisPro program.²⁶ The crystal structures were determined by the *ab initio* method using the Superflip program²⁷ and refined by least squares using the SHELXL program.²⁸ All non-hydrogen atoms were refined in the anisotropic approximation. Hydrogen atoms were specified geometrically with the thermal parameters $U_{iso}(H) = 1.2U_{eq}$ of the corresponding C and N atoms. The main crystallographic data and refinement parameters of the structure of salt **1** are presented in Table 1.

The crystals of compound **2** were identified by X-ray diffraction analysis, which showed their complete identity with salt α '- $ET_2N(CN)_2 \cdot 2H_2O$ earlier synthesized and described by us.¹⁸

The crystallographic data for salt **1** were deposited with the Cambridge Crystallographic Data Center (CIF file CCDC 1439588) and can be obtained free of charge at www.ccdc.cam.ac.uk/getstructures.

Measurement of conductivity. The conductivity of the crystals was measured in the conducting plane of the crystal by the standard four-contact method on an automated setup with dc in a temperature range of 300–100 K. Platinum wire contact ($d = 10 \mu\text{m}$) were glued to the crystal using the DOTITE XC-12 graphite paste.

The authors are grateful to L. I. Buravov for measuring conductivity.

This work was financially supported by the Russian Foundation for Basic Research (Project Nos. 14-03-00119 and 15-02-02723) and the NNIO (Project No. KA 1652/4-1).

References

1. E. Coronado, P. Day, *Chem. Rev.*, 2004, **104**, 5419.
2. T. Enoki, A. Miyazaki, *Chem. Rev.*, 2004, **104**, 5449.
3. L. Ouahab, in *Organic Conductors, Superconductors and Magnets: From Synthesis to Molecular Electronics*, Eds L. Ouahab, E. Yagubskii, Kluwer Academic, Dordrecht—Boston—London, 2003, p. 99.
4. A. Audouard, V. N. Laukhin, L. Brossard, T. G. Prokhorova, E. B. Yagubskii, E. Canadell, *Phys. Rev.*, 2004, **B 69**, 144523.
5. M. Kurmoo, A. W. Graham, P. Day, S. J. Coles, M. B. Hursthouse, J. L. Caulfield, J. Singleton, F. L. Pratt, W. Hayes, L. Ducasse, P. Guionneau, *J. Am. Chem. Soc.*, 1995, **117**, 12209.
6. T. Otsuka, A. Kobayashi, Y. Miyamoto, J. Kiuchi, S. Nakamura, N. Wada, E. Fujiwara, H. Fujiwara, H. Kobayashim, *J. Solid State Chem.*, 2001, **159**, 407.
7. E. Ojima, H. Fujiwara, K. Kato, H. Kobayashi, H. Tanaka, A. Kobayashi, M. Tokumoto, P. Cassoux, *J. Am. Chem. Soc.*, 1999, **121**, 5581.
8. S. Uji, H. Shinagawa, T. Terashima, T. Yakabe, Y. Terai, M. Tokumoto, A. Kobayashi, H. Tanaka, H. Kobayashi, *Nature*, 2001, **410**, 908.
9. H. Fujiwara, H. Kobayashi, E. Fujiwara, A. Kobayashi, *J. Am. Chem. Soc.*, 2002, **124**, 6816.
10. J. W. Raebiger, J. L. Manson, R. D. Sommer, U. Geiser, A. L. Rheingold, J. S. Miller, *Inorg. Chem.*, 2001, **40**, 2578.
11. J. Schlueter, U. Geiser, J. L. Manson, *J. Phys. IV France*, 2004, **114**, 475.
12. B. H. Ward, G. E. Granroth, J. B. Walden, K. A. Abboud, M. W. Meisel, P. G. Rasmussen, D. R. Talham, *J. Mater. Chem.*, 1998, **8**, 1373.
13. J. A. Shlueter, J. L. Manson, U. Geiser, *Inorg. Chem.*, 2005, **44**, 3194.
14. N. D. Kushch, A. V. Kazakova, A. D. Dubrovskii, G. V. Shilov, L. I. Buravov, R. B. Morgunov, E. V. Kurganova, Y. Tanimoto, E. B. Yagubskii, *J. Mater. Chem.*, 2007, **17**, 4407.
15. V. N. Zverev, M. V. Kartsovnik, W. Biberacher, S. S. Khasanov, R. P. Shibaeva, L. Ouahab, L. Toupet, N. D. Kushch, E. B. Yagubskii, E. Canadell, *J. Phys. Rev.*, 2010, **B82**, 155123.
16. E. B. Yagubskii, N. D. Kushch, A. V. Kazakova, L. I. Buravov, V. N. Zverev, A. I. Manakov, S. S. Khasanov, R. P. Shibaeva, *JETP Lett. (Engl. Transl.)*, 2005, **82**, 93 [*Pis'ma v Zh. Eksp. Teor. Fiz.*, 2005, **82**, 99].
17. N. D. Kushch, A. V. Kazakova, L. I. Buravov, A. N. Chekhlov, A. D. Dubrovskii, E. B. Yagubskii, E. Canadell, *J. Solid State Chem.*, 2009, **182**, 617.
18. A. V. Kazakova, N. D. Kushch, A. N. Chekhlov, A. D. Dubrovskii, E. B. Yagubskii, K. V. Van, *Russ. J. Gen. Chem. (Engl. Transl.)*, 2008, **78**, 6 [*Zh. Obshch. Khim.*, 2008, **78**, 6].
19. N. D. Kushch, E. B. Yagubskii, M. V. Kartsovnik, L. I. Buravov, A. D. Dubrovskii, A. N. Chekhlov, W. Biberacher, *J. Am. Chem. Soc.*, 2008, **130**, 7238.
20. O. M. Vyaselev, N. D. Kushch, E. B. Yagubskii, *J. Exp. Theor. Phys. (Engl. Transl.)*, 2011, **140**, 961 [*Zh. Eksp. Teor. Fiz.*, 2011, **140**, 961].
21. O. M. Vyaselev, R. Kato, H. M. Yamamoto, A. Kobayashi, L. V. Zorina, S. V. Simonov, N. D. Kushch, E. B. Yagubskii, *Crystals*, 2012, **2**, 224.
22. T. Mori, H. Mori, Sh. Tanaka, *Bull. Chem. Soc. Jpn.*, 1999, **72**, 179.
23. P. Guionneau, C. J. Kepert, G. Bravic, D. Chasseau, M. R. Truter, M. Kurmoo, P. Day, *J. Synth. Met.*, 1997, **86**, 1973.
24. A. Nag, P. J. Schmidt, W. Schnick, *Chem. Mater.*, 2006, **18**, 5738.
25. J. A. Schlueter, J. L. Manson, U. Geiser, *C. R. Chimie*, 2007, **10**, 101.
26. *CrysAlisPro, Agilent Technologies, Version 1.171.35.21*, 2012.
27. L. Palatinus, G. Chapuis, *J. Appl. Crystallogr.*, 2007, **40**, 786.
28. G. M. Sheldrick, *Acta Crystallogr., Sect. A*, 2008, **64**, 112.

Received December 4, 2015